Pengzhen Duan[1], Hanying Li[1], Zhibang Ma[2], Jingyao Zhao[1], Ashish Sinha[3], Peng Hu[4], Haiwei Zhang[1], Yanjun Cai[1], Youfeng Ning[1], R. Lawrence Edwards[5], and Hai Cheng[1,6]

[1]Institute of Global Environmental Change, Xi'an Jiaotong University, Xi'an, China

[2]Key Laboratory of Cenozoic Geology and Environment, Institute of Geology and Geophysics, Chinese Academy of Sciences, Beijing, China

[3]Department of Earth Science, California State University, Dominguez Hills, Carson, USA

[4]Institute of Atmospheric Physics, Chinese Academy of Sciences, Beijing, China

[5]Department of Earth and Environmental Sciences, University of Minnesota, Minneapolis, USA

[6]State Key Laboratory of Loess and Quaternary Geology, Institute of Earth Environment, Chinese Academy of Sciences, Xi'an, China

Corresponding author: Hanying Li (hanyingli@xjtu.edu.cn) and Hai Cheng (cheng021@xjtu.edu.cn)

Key Points:

- Annual laminated speleothem ^{18}O record from North China manifests a two-stage 8.2 ka event superimposed by three positive excursions
- High consistency of speleothem records from North and central China on interdecadal to multidecadal timescales indicates a common driver
- The climate forcing for the termination process is different from the early and middle stages of the 8.2 ka event

Abstract

The 8.2 ka event has been extensively studied, whereas its structure is ambiguous in North China. Here we present a high-resolution (~1 year) ^{18}O record of annual laminated speleothem from Beijing to characterize the detailed variability across this event in North China. Our record indicates a dry 8.2 ka event spanning 8.254 8.107 ka BP with a two-stage structure superimposed by three prominent positive excursions. The identical structure of speleothem ^{18}O records between North and central China during the event suggests a common forcing/response in East China, whereas the progressively increased offset between their average values may reflect changes in moisture source or rainout effect. A close comparison with the Greenland ice core records suggest a strong linear response of the Asian summer monsoon to the North Atlantic climate changes across the early and middle stages of the event, but a different mechanism in the termination process.

Plain Language Summary

This study presents a new high-resolution (~1 year) speleothem ^{18}O record from Beijing, North China to characterize the timing and structure of the 8.2 ka event. Our record reveals a two-stage structure superimposed by three prominent "V-shape" excursions across the 8.2 ka event. The almost exact covariation of records from North and central China on interdecadal to multidecadal scales suggests a coherent Asian summer monsoon (ASM) changes in response to the same forcing. However, a close comparison between them shows a progressively increased offset between their average ^{18}O values, presumably caused by changes in moisture source and/or rainout processes associated with the ASM circulations. Within the dating uncertainty, a -15 years shift of the Greenland ice core chronology around the 8.2 ka event is proposed, so that the Greenland ice core and Chinese speleothem ^{18}O records are synchronized regarding the three "V-shape" excursions in the 8.2 ka event. This is in turn consistent with the dynamic mechanism—fast ASM weakening in response to the North Atlantic cooling. Of note, however, are the event termination processes that appear to be distinct between Greenland ice core and Chinese speleothem records, implying another forcing mechanism.

1 Introduction

The 8.2 ka event, as the most prominent abrupt cold event within the Holocene registered initially in the Greenland ice core records (Thomas et al., 2007), has been widely revealed by a large number of marine and terrestrial archives and dated to ~8.3–8.0 ka BP (thousand years before present, present = 1950 CE) with a duration of 150–200 years (Figure S1) (e.g., Alley et al., 1997; Thomas et al., 2007; Cheng et al., 2009a; Liu et al., 2013; Morrill et al., 2013; P. Duan et al., 2021). This event has been generally attributed to an interruption (or slowdown) of the Atlantic Meridional Overturning Circulation (AMOC) resulting from a large freshwater influx into the North Atlantic, causing a series of chain responses of climate globally (e.g., Alley et al., 1997; Barber et al., 1999; Ellison et al., 2006; Matero et al., 2017).

In the Asian summer monsoon (ASM) domain, speleothem proxies from central-South China suggested that the 8.2 ka event was associated with a weak monsoon interval attendant with prevalent drought (Cheng et al., 2009a; Liu et al., 2013; Liu et al., 2015; Liu & Hu, 2016). The internal structure of the event has been well characterized by, for example, 3-year resolved and well-dated (multidecadal on 2 uncertainty) speleothem oxygen isotope (^{18}O) records from Dongge Cave in South China (Figure S1), as a prominent two-stage event (Cheng et al., 2009a). Other two high-resolution speleothem ^{18}O records from Heshang Cave (<1 year, Liu et al., 2013) and nearby Qingtian Cave (~3 years, Liu et al., 2015) (Figure S1) in central China, both based on annual band counted relative chronologies, show excellent agreement with each other both in duration and structure, and correlate closely with the high-resolution Greenland ice core records. In North China, although speleothem ^{18}O records have also revealed positive excursions near 8.2 ka BP (Dong et al., 2018; Tan et al., 2020; W. Duan et al., 2021), detailed constrains on the structure and duration are still absent

because of the limits on dating precision and/or temporal resolution. Additionally, though the speleothem ^{18}O record from Nuanhuo Cave in Northeast China is highly resolved (~2 years) with the age controlled by annually-laminated band around the 8.2 ka event, the structure of the event is rather ambiguous (Wu et al., 2012). Hence, it remains important to reconstruct high-resolution and precisely dated records to characterize the manifestation of the 8.2 ka event in North China in order to comprehensively understand its timing, structure, relationship to South China, and the underlying mechanism(s). Moreover, the ecosystem and economic development in North China are highly dependent on the hydroclimatic condition, thus it is crucial to understand the paleoclimate variations under various forcings such as the freshwater influx in the North Atlantic which possibly triggered the 8.2 ka event and could be one of the future scenarios (e.g., Aguiar et al., 2020).

In this study, we reconstruct high temporal resolution speleothem ^{18}O record from Huangyuan Cave in Beijing, North China, to characterize interdecadal to multidecadal hydroclimatic variations over the Circum-Bohai Sea Region (CBSR) during 8.4–8.0 ka BP. Precise U-Th dates and annual band counting results are combined to establish the chronology of the record. Our new record document a two-stage 8.2 ka event superimposed by three "V-shape" heavy ^{18}O anomalies, and a recovery overshoot ensuing the termination of this event. Compared with other high-resolution paleoclimatic records, we show the identical hydroclimatic patterns in North and central China, and the casual link between the ASM and the North Atlantic climate on interdecadal to multidecadal scales across the 8.2 ka event.

2 Materials and Methods

2.1 Cave Settings and Modern Climatology

The Huangyuan Cave (39°42 N, 115°54 E) is located at Fangshan District of Beijing, North China, close to Kulishu (39°41 N, 119°39 E) and Shihua (39°47 N, 115°56 E) Caves (Figure S1). The cave was developed in the Middle Proterozoic dolomite (Ma et al., 2012; Duan et al., 2014). Speleothem BH-2, collected from Huangyuan Cave in 2002, is ~170 mm high and ~50 mm wide. In this study, we focus on the section from 15 to 48 mm, corresponding to 8.38 8.06 ka BP.

The local mean annual temperature and precipitation is 12.2 °C and 540 mm, respectively, during 1998 and 2010 at the Fangshan meteorological station (Figure 1). Around 80 % annual rainfall occurs during the summer monsoon season (June to September: JJAS) with July–August (JA) accounting for ~56 % of annual amount. The monsoonal rainfall variability in the Huangyuan Cave area well represents the precipitation pattern over a large part of North China, especially the CBSR (114–124 °E, 36–41 °N) in both JJAS and JA (Figures 1 and S2). Given the high resemblance of JA regional precipitation with JJAS (r = 0.89, Figure S2), we focus on JA to further investigate the interannual hydrological dynamic over the CBSR. The bulk of rainfall concentratedly falls during

JA, when the intensified monsoon wind brings abundant moisture into North China (Figure 1). The Yanshan and Taihang mountains create the windward precipitation conditions around Beijing (Lei et al., 2020), contributing to the concentrated JA rainfall. When the southerly monsoonal wind weakens, anomalous northeasterly moisture flux brings drier air mass into the CBSR, leading to less rainfall over the study area (Figure 1). On decadal to multidecadal scales, the precipitation variability over the CBSR appears to be paced by the Pacific Decadal Oscillation (PDO), suggesting an important role of the Pacific on regulating the ASM (Figure 1) (e.g., Yu, 2013; Qian & Zhou, 2014; Li et al., 2017). Whereas the teleconnection of the CBSR precipitation with the Atlantic multidecadal oscillation (AMO) remains ambiguous (Figure 1), likely implying more complex mechanism.

Precipitation ^{18}O ($^{18}O_p$) values over Huangyuan Cave and the neighboring region exhibit large seasonal variations with the lowest in winter (< -10 ‰), the highest in spring (> -4 ‰), and median in summer (between -6 and -10 ‰) according to Global Network of Isotopes in Precipitation (GNIP, https://www.iaea.org/services/networks/gnip) dataset, IsoGSM simulations (Yoshimura et al., 2008), and monitoring results (Duan et al., 2014) (Figure S3a). Modern monitoring results showed that the seasonal ^{18}O variations of drip water ($^{18}O_{drip}$) in nearby Shihua Cave was quite limited (-8.5 -9.5 ‰) (Duan et al., 2016). Noticeably, the $^{18}O_{drip}$ value is not only close to the annual precipitation amount-weighted $^{18}O_p$ outside Shihua Cave obtained from monitoring work, but also correlated well with the IsoGSM-simulated annual precipitation amount-weighted $^{18}O_p$ at Huangyuan Cave (Figure S3b). Given the fact that summer precipitation accounts for 80 % annual amount, the $^{18}O_{drip}$ in the cave aquifer mainly inherits the $^{18}O_p$ of summer monsoon rainfall or effectively the most intense rainfall in JA (Figure S4d). The significant negative correlation between summer rainfall over the CBSR and $^{18}O_p$ at the cave site suggests that the "amount effect" of regional precipitation (Zhao et al., 2019) plays a critical role in modulating the $^{18}O_p$ (Figures S4 and S5). Unlike the large-scale heterogeneous spatial pattern of precipitation amount, the $^{18}O_p$ at the study site is positively correlated with $^{18}O_p$ almost over the entire ASM domain (Figure S4a), indicating a common forcing on the ASM $^{18}O_p$— variations of the large-scale atmospheric circulation, referred as the ASM intensity (e.g., Cheng et al., 2019, 2021b). The composite spatial patterns of difference between extreme high and low $^{18}O_p$ years show anomalous less precipitation, increased descending air motion, and anomalous northerly and northeasterly low-level wind (850 hPa), further demonstrating that reduced convection and less rainfall over the CBSR are coincident causally with increased $^{18}O_p$ in this region (Figures 1 and S5).

2.2 ^{230}Th Dating and Stable Isotope Analysis

A total of eleven ^{230}Th dates (Table S1) were determined at the Isotope Laboratory of University of Minnesota using Thermo-Finnigan Neptune multi-collector

inductively coupled plasma mass spectrometers. The methods are described in detail in Cheng et al. (2013). We followed standard chemistry procedures to separate uranium and thorium (Edwards et al., 1987). A triple-spike (^{229}Th-^{233}U-^{236}U) isotope dilution method was employed to correct instrumental fractionation and determine U-Th isotopic ratios and concentrations. The instrumentation, standardization and half-lives are reported in Cheng et al. (2013).

The ^{18}O values were determined on a Thermo-Scientific MAT-253 isotope ratio mass spectrometer equipped with Kiel IV carbonate device. The powdered subsamples were contiguously drilled along the central growth axis using a micromill device and reacted with ~103 % phosphoric acid at 70 °C. Liberated CO_2 gas was measured with working CO_2 standard gas whose value has been calibrated with international standards. All results are reported relative to the Vienna Pee Dee Belemnite (VPDB) and their precision at 1 level is better than 0.1 ‰.

2.3 Annual Band Counting and Age Model

Confocal Laser Fluorescent Microscopy (CLFM) was used to observe clear annual bands, each of which comprises paired light and dark lamina (Figures 2 and S6). The detailed method is described in Zhao & Cheng (2017). In this study, each visible bright band was counted as one year. To reduce counting error, six times counting were performed to obtain the mean values and associated uncertainties.

Firstly, we constrain the chronology between 16–43 mm through anchoring annual band counting to the encompassed seven ^{230}Th dates (Table S1) using the least square method (Domínguez-Villar et al., 2012). Theoretically, the resultant uncertainty comes from two main sources: (a) layer counting (LC) uncertainty (12 years (2) based on 6 times of counting), (b) the accuracy in anchoring the lamina counting to the radiometric dates (A, 28 years). Finally, the combined error ( ) is ~30 years (2), calculated by the following formula:

$$=\sqrt{(LC^2 + A^2)}$$

The obtained floating chronology results are consistent with the ^{230}Th dates within uncertainties (Figure S6), indicating the robustness of above method.

To establish the consecutive chronology for the entire record, all above fitting age results for each band in 16–43 mm (corresponding to 8.077–8.324 ka BP) with uncertainties and the other four ^{230}Th dates (Table S1) in the remnant study section are input to Oxcal algorithm. The output results show negligible offset in comparison with floating chronologies for 8.324–8.077 ka BP and ^{230}Th dates within uncertainties (Figure S6).

3 Results

The BH-2 ^{18}O record, covering 8.38–8.06 ka BP, contains 350 data with a mean temporal resolution of 1 year. The ^{18}O ranges from -7.06 ‰ to -11.54

‰ with a mean value of -9.22 ‰. One remarkable feature of the ^{18}O record is the pronounced positive excursion near 8.2 ka BP (Figure 2), similar with the observation in a speleothem ^{18}O record from nearby Kulishu Cave (W. Duan et al., 2021) (Figures S7). This coherency suggests that the influence of kinetic fractionations is likely insignificant and the speleothem carbonate deposition process is close to equilibrium (Dorale & Liu, 2009). Hence, the BH-2 ^{18}O signal reflects the changes in $^{18}O_{drip}$ originating from the $^{18}O_p$, which is in turn related to the regional hydroclimatic variations in general.

4 Discussion

4.1 Interpretation of the Speleothem ^{18}O

The negative correlation between summer $^{18}O_p$ and the CBSR precipitation amount, and the broad $^{18}O_p$ consistency over the ASM domain (Figure S4) suggest the important impacts of local precipitation amount and large-scale ASM circulation on $^{18}O_p$ in Beijing area, respectively. Since speleothem BH-2 was deposited in approximately equilibrium conditions as aforementioned, its ^{18}O signal generally inherits from the $^{18}O_p$ in the summer monsoon season. This view is supported by aforementioned observations that the $^{18}O_{drip}$ variation is small and close to the mean $^{18}O_p$ of the rainy summer and the annual amount-weighted $^{18}O_p$ from monitoring (Duan et al., 2014) and IsoGSM simulation (Figure S3). Therefore, in this study we use the BH-2 ^{18}O proxy to indicate the variations of regional rainfall and large-scale $^{18}O_p$ in East Asia: depleted ^{18}O corresponds to more rainfall over the CSBR and intensified ASM, and vice versa (e.g., Ma et al., 2012; Li et al., 2017; Cheng et al., 2019, 2021b; W. Duan et al., 2021).

4.2 The Timing and Structure of the 8.2 ka Event in North China

The BH-2 ^{18}O record reveals interdecadal to multidecadal dry ($> +1$) (Liu et al., 2013) or pluvial (< -1) oscillations between 8.4 and 8.0 ka BP without a long-term trend (Figure 2b). One of noticeable features of this record is a switch from small (1) to larger (>1) variation episodes commencing ~8.25 ka BP (Figure 2). The overall higher ^{18}O interval between 8.25–8.0 ka BP is synchronous with the anomalous higher ^{18}O values at around 8.2 ka BP documented in nearby Kulishu Cave within age uncertainties (Figures S1) (W. Duan et al., 2021), supporting a regional aridity or weakened ASM. If defining the onset and termination with higher ^{18}O than the mean of entire record for lasting more than 20 consecutive years, the 8.2 ka event in the BH-2 record is pinpointed to 8.254–8.107 ka BP (Figure 2). These timing and duration are broadly consistent with Greenland ice cores (8.247–8.086 ka BP) (Thomas et al., 2007) and speleothem records from South America (8.21–8.06 ka BP: Cheng et al., 2009a) and central China (8.25–8.10 ka BP: Liu et al., 2013) within age uncertainties. Taking advantages of annual band chronology and high-resolution of the BH-2 record, we characterize the detailed structure of the 8.2 ka event in North China. Consistent with previous findings (Cheng et al., 2009a), the

8.2 ka event mainly consists of two stages, namely the Stage I and Stage II, and in the BH-2 ^{18}O record the two stages is divided at ~8.15 ka BP when the ^{18}O bounced back to the mean value (Figure 2). Notably, three multidecadal "V-shape" positive excursions are prominent during the 8.2 ka event in the BH-2 ^{18}O record: two excursions (8.254–8.189 and 8.189–8.156 ka BP) occurred in the Stage I and one (8.156–8.127 ka BP) in the Stage II (Figure 2). The ^{18}O maxima of these excursions are -8.5 ‰, -7.1 ‰ and -8.1 ‰, respectively, with the middle one representing the most pronounced ^{18}O enrichment in the entire record. Intriguingly, the structure of three excursions was also observed in the gray-scale record from the Cariaco Basin (Hughen et al., 1996) and Cl value record from the Cuban sinkhole (Peros et al., 2017) (Figure S1), presumably suggesting a causal link among these subevents in different climate systems.

The post-event variations are prominently characterized by a fast rebound back to the wet condition (green shading in Figure 2), including an abrupt interdecadal excessive rebound (i.e., overshoot) attaining the lowest ^{18}O values (-11.5 ‰) of the entire record (Figure 2). Of note is that the overshoot is also observed in other speleothem records in the ASM domain, such as the Kulishu (W. Duan et al., 2021) and Lianhua (Dong et al., 2018) records (Figure S1), suggesting a major pluvial episode prevailing across a large part of North China. Furthermore, this strong pluvial overshoot appears to coincide with the post-event temperature overshoot inferred by an annual band constrained lake sediment record from Austria in the North Atlantic region (Andersen et al., 2017), indicating a tight climatic link between the ASM and the North Atlantic climate systems in this period.

4.3 Detailed Comparison of the 8.2 ka Event between North and Central China

High-resolution speleothem ^{18}O records with annual band constraints from central China (HS-4 from Heshang Cave, Liu et al., 2013) and North China (BH-2) allow us to further explore the temporal-spatial pattern of the 8.2 ka event in East China. The comparison between two records (~1200 km away from each other) exhibits significant similarity in the onset, termination, and structure of the 8.2 ka event, particularly the three "V-shape" positive ^{18}O excursions (Figure 3a). This consistency is verified by the significant correlation ($r = 0.69$) (Figure 3a), or a higher correlation coefficient ($r = 0.75$) when the chronology of HS-4 is shifted by -6 years (Figure 3b) within its absolute age uncertainty (>120 years). This high-degree resemblance suggests a strict coherent climate response from both North and central China to the same forcing during the 8.2 ka event on interdacadal to multidecadal timescales, or a manifestation of the large spatial-scale consistency of the ^{18}O variability across the event.

Despite the high similarity between the ^{18}O variation patterns in North and central China, their differences increase progressively in terms of the mean speleothem ^{18}O values in three episodes (i.e., Stage I, Stage II and the overshoot) (Figure 3). In the Stage I, the absolute ^{18}O values of the two records are virtually identical with mean values of -8.51 ‰ (the BH-2 record) and -8.61 ‰ (the HS-4 record), respectively. In the Stage II, the difference increases to 0.53

‰ with more depleted ^{18}O in BH-2 from North China relative to HS-4 from central China. In the overshoot period, the difference reaches 1 ‰ (Figure 3). These observations may plausibly indicate that hydroclimate in North China is more sensitive than central China to the same climatic disturbance. One of possible explanations lies in the amplified response of North China to the progressive warming from the Stage I to the overshoot, that is, the precipitation amount or the "rainout effect" on the $^{18}O_p$ increased between North and central China (Hu et al., 2008). Alternatively, this may imply that the portion of the southerly moisture from the tropical oceans in the annual precipitation, which is typically lower in ^{18}O value, increased more in North China than in central China during the warming episodes (Cheng et al., 2009b; Tan, 2014; Hu et al., 2019; Zhang et al., 2021b).

4.4 Teleconnection of Multidecadal ASM Variation to the North Atlantic Climate

It is generally an accepted hypothesis that the 8.2 ka event was triggered by a large amount freshwater influx into the North Atlantic, which in turn induced a slowdown of the AMOC, resulting significant reduce of the heat transport from low-latitude to the North Atlantic and causing cooling in the circum-North Atlantic region (e.g., Alley et al., 1997; Barber et al., 1999; Jennings et al., 2015; Wagner et al., 2013). This abrupt climate signal propagated fast via atmospheric processes to global extent, including the ASM realm (Cheng et al., 2009a; Liu et al., 2013).

The speleothem BH-2 and Greenland ice core records (Thomas et al., 2007) are all constrained by annual band counting, thus allow us to explore their teleconnections in detail. The direct comparison between the BH-2 and Greenland ice core ^{18}O records shows that the dips at 8.215, 8.175 and 8.137 ka BP in the BH-2 record seems to be synchronous to the corresponding peaks in the Greenland ice core record (Figures 4a and 4c), implying a correlation of the warming in Greenland (Thomas et al., 2007) with the dry or weakened ASM in North China. This teleconnection is contrary to the conventional wisdom that cooling in the North Atlantic is coincident with the weak ASM both empirically (e.g., Gupta et al., 2003; Wang et al., 2005; Cheng et al., 2009a) and theoretically (e.g., Chiang & Bitz, 2005; Zhang & Delworth, 2005; Broccoli et al., 2006; Schneider et al., 2014; Wang et al., 2017). A recent state-of-the-art strategy of the correlation between Chinese speleothem and Greenland ice core ^{18}O records suggests a synchronous onset of millennial events between cooling in Greenland and weakening in the ASM, such as the Young Dryas (Cheng et al., 2020) and Heinrich Stadial 4 (Cheng et al., 2021a). Following the same strategy, it is reasonable to assume that the onset of the 8.2 ka event is also synchronous between the ASM and Greenland ^{18}O records. This then requires a -15 years shift of the Greenland ice core ^{18}O record, which is well within the quoted 45-year age uncertainty of the Greenland record around this period (Rasmussen et al., 2014). Correspondingly, we shift the composite Greenland ice core ^{18}O record -15 years without changing the relative ages (Figure 4). In this

new chronological framework, the onset and three "V-shape" dips of the 8.2 ka event in the Asian monsoon records coincide remarkably with the Greenland ice core composite ^{18}O record, reinforcing the view that the North Atlantic cooling triggered by the AMOC change will result in the immediate ASM weakening as a response (e.g., Liu et al., 2013; Cheng et al., 2020, 2021a). In theory, current dating uncertainties of the Greenland ice cores (~45 years), the HS-4 (>100 years) and BH-2 (~30 years) still leave room for allowing different correlations within decadal to multi-decadal uncertainties. However, from climate dynamic point of view, we prefer the new correlation framework mentioned above (Figure 4), because this is consistent with the dynamics that the abrupt climatic signals from the North Atlantic can rapidly propagate through atmospheric processes globally, including to the ASM domain (Liu et al., 2013; Duan et al., 2016) as well as Antarctica (Ruth et al., 2007; Markle et al., 2017; Cheng et al., 2020).

In the -15-year shift scenario, it is intriguing that the termination processes of the 8.2 ka event appears to be decoupled in the Greenland and the ASM proxy records. In the late part of the Stage II, BH-2 and HS-4 ^{18}O values decrease persistently from ~8.140 ka BP and almost rebound back to pre-event level at ~8.125 ka BP (Figure 4). In contrast, the Greenland ice core ^{18}O in the termination period seems taking longer time to return to the pre-event condition. As a result, the internal structure in the termination processes is apparently distinct between Chinese speleothem and Greenland ice core records. More evidences for the interregional similarities in the early and middle 8.2 ka event and the dissimilarities in the termination processes are observed in a number of paleoclimate records from various climate systems (Figure S1) (P. Duan et al., 2021), likely suggesting different dynamic mechanism(s) in two intervals (P. Duan et al., 2021). It seems that the distinct termination processes (Figure 4) imply a low-middle latitude to high latitude directionality for the climate signal propagation, which is akin to the termination of millennial-scale abrupt events, such as the Younger Dryas (Cheng et al., 2020) and Heinrich Stadial 4 (Cheng et al., 2021a), possibly indicating that the initial trigger (precursor events) of the termination resided out of the North Atlantic (Cheng et al., 2020, 2021a; Zhang et al., 2021a).

5 Conclusions

The new high-resolution (~1 year) and precisely dated (combination of annual band counting and ^{230}Th dates) speleothem ^{18}O record from Beijing, North China characterizes in detail the ASM variability within the 8.2 ka event. This record reveals an overall arid 8.2 ka event lasting from 8.254 to 8.107 ka BP characterized by a two-stage structure with three distinctive heavy excursions and a post-event overshoot ensuing the event termination. Comparison with speleothem record from central China indicates remarkably coherent climate variations in East Asia in response to the same climate forcing, but their difference of the average ^{18}O values gradually increases from the Stage I to the overshoot, likely dominated by changes in moisture source or rainout effect linked to the large-scale ASM circulation variations. Based on the synchronicity

between the North Atlantic cooling and the ASM waning, we propose a -15-year chronology shift for the Greenland ice core records. In this new chronology framework, the apparent consistency regarding the three "V-shape" excursions in the Greenland and Chinese records suggests a precisely linear climate response of the ASM to the North Atlantic on interdecadal scale. Nevertheless, this conspicuous coherency vanishes in the termination processes, probably indicating different mechanism.

Acknowledgments

This work was supported by the National Natural Science Foundation of China grants (41731174, 41888101 and 42150710534 to H.C.). We specially thank Ming Tan, Wuhui Duan, Jiapeng Miao and Xian Wu for their helpful suggestions and kind help on the modern climate analysis.

Data Availability Statement

The ERA5 Reanalysis is obtained from https://cds.climate.copernicus.eu. The speleothem data presented in this study will be available in the public paleoclimate database of NOAA after the manuscript is accepted.

References

Aguiar, W., Meissner, K. J., Montenegro, A., Prado, L., Wainer, I., Carlson, A. E., et al. (2021). Magnitude of the 8.2 ka event freshwater forcing based on stable isotope modelling and comparison to future Greenland melting. *Scientific Reports, 11*, 1–10. https://doi.org/10.1038/s41598-021-84709-5

Alley, R. B., Mayewski, P. A., Sowers, T., Stuiver, M., Taylor, K. C., & Clark, P. U. (1997). Holocene climatic instability: a prominent, widespread event 8200 yr ago. *Geology, 25*, 483–486. https://doi.org/10.1130/0091-7613(1997)025<0483:HCIAPW>2.3.CO;2

Andersen, N., Lauterbach, S., Erlenkeuser, H., Danielopol, D. L., Namiotko, T., Hüls, M., et al. (2017). Evidence for higher-than-average air temperatures after the 8.2 ka event provided by a Central European ^{18}O record. *Quaternary Science Reviews, 172*, 96–108. http://dx.doi.org/10.1016/j.quascirev.2017.08.001

Barber, D. C., Dyke, A., Hillaire-Marcel, C., Jennings, A. E., Andrews, J. T., Kerwin, M. W., et al. (1999). Forcing of the cold event of 8,200 years ago by catastrophic drainage of Laurentide lakes. *Nature, 400*, 344. https://doi.org/10.1038/22504.

Broccoli, A. J., Dahl, K. A., & Stouffer, R. J. (2006). Response of the ITCZ to Northern Hemisphere cooling. *Geophysical Research Letters, 33*(1), L01702. https://doi.org/10.1029/2005GL024546.

Cheng, H., Edwards, R. L., Shen, C. C., Polyak, V. J., Asmerom, Y., Woodhead, J., et al. (2013). Improvements in ^{230}Th dating, ^{230}Th and ^{234}U half-life values, and U-Th isotopic measurements by multi-collector inductively coupled plasma mass spectrometry. *Earth Planet Science Letters, 371–372*, 82–91.

https://doi.org/10.1016/j.epsl.2013.04.006

Cheng, H., Fleitmann, D., Edwards, R. L., Wang, X., Cruz, F. W., Auler, A. S., et al. (2009a). Timing and structure of the 8.2 kyr B.P. event inferred from ^{18}O records of stalagmites from China, Oman, and Brazil. *Geology, 37*, 1007–1010. https://doi.org/10.1130/G30126A.1

Cheng, H., Edwards, R. L., Broecker, W. S., Denton, G. H., Kong, X., Wang, X., et al. (2009b). Ice age terminations. *Science, 326*(5950), 248–252. https://doi.org/10.1126/science.1177840

Cheng, H., Xu, Y., Dong, X., Zhao, J., Li, H., Baker, J., et al. (2021a). Onset and termination of Heinrich Stadial 4 and the underlying climate dynamics. *Communications Earth & Environment, 2*(1), 1–11. https://doi.org/10.1038/s43247-021-00304-6

Cheng, H., Zhang, H., Cai, Y., Shi, Z., Yi, L., Deng, C., Perez-Mejías, C., et al. (2021b). Orbital-scale Asian summer monsoon variations: Paradox and exploration. *Science China Earth Sciences, 64*(4), 529–544. https://doi.org/10.1007/s11430-020-9720-y

Cheng, H., Zhang, H., Spotl, C., Baker, J., Sinha, A., Li, H., et al. (2020). Timing and structure of the Younger Dryas event and its underlying climate dynamics. *Proceedings of the National Academy of Sciences of the United States of America, 117*, 23408–23417. https://doi.org/10.1073/pnas.2007869117

Cheng, H., Zhang, H., Zhao, J., Li, H., Ning, Y., & Kathayat, G. (2019). Chinese stalagmite paleoclimate researches: A review and perspective. *Science China Earth Sciences, 62*(10), 1489–1513. https://doi.org/10.1007/s11430-019-9478-3

Chiang, J. C., & Bitz, C. M. (2005). Influence of high latitude ice cover on the marine Intertropical Convergence Zone. *Climate Dynamics, 25*(5), 477–496. https://doi.org/10.1007/s00382-005-0040-5

Domínguez-Villar, D., Baker, A., Fairchild, I. J., & Edwards, R. L. (2012). A method to anchor floating chronologies in annually laminated speleothems with U-Th dates. *Quaternary Geochronology, 14*, 57–66. https://doi.org/10.1016/j.quageo.2012.04.019

Dong, J., Shen, C. C., Kong, X., Wu, C. C., Hu, H. M., Wang, Y., et al. (2018). Rapid retreat of the East Asian summer monsoon in the middle Holocene and a millennial weak monsoon interval at 9 ka in northern China. *Journal of Asian Earth Sciences, 151*, 31–39. https://doi.org/10.1016/j.jseaes.2017.10.016

Dorale, J. A., & Liu, Z. (2009). Limitations of Hendy test criteria in judging the paleoclimatic suitability of speleothems and the need for replication. *Journal of Cave and Karst Studies, 71*, 73–80.

Duan, P., Li, H., Sinha, A., Voarintsoa, N. R. G., Kathayat, G., Hu, P., et al. (2021). The timing and structure of the 8.2 ka event revealed through

high-resolution speleothem records from northwestern Madagascar. *Quaternary Science Reviews, 268*, 107104. https://doi.org/10.1016/j.quascirev.2021.107104

Duan, W., Ma, Z., Tan, M., Cheng, H., Edwards, R. L., Wen, X., et al. (2021). Timing and structure of Early-Holocene climate anomalies inferred from north Chinese stalagmite records. *The Holocene*, *31*, 1777–1785. https://doi.org/10.1177/09596836211033218

Duan, W., Ruan, J., Luo, W., Li, T., Tian, L., Zeng, G., et al. (2016). The transfer of seasonal isotopic variability between precipitation and drip water at eight caves in the monsoon regions of China. *Geochimica et Cosmochimica Acta*, *183*, 250–266. http://dx.doi.org/10.1016/j.gca.2016.03.037

Duan, W., Tan, M., Ma, Z., & Cheng, H. (2014). The palaeoenvironmental significance of ^{13}C of stalagmite BH-1 from Beijing, China during Younger Dryas intervals inferred from the grey level profile. *Boreas*, *43*, 243–250. https://doi.org/10.1111/bor.12034

Edwards, R. L., Chen, J. H., & Wasserburg, G. J. (1987). ^{238}U-^{234}U-^{230}Th-^{232}Th systematics and the precise measurement of time over the past 500,000 years. *Earth Planet Science Letters*, *81*, 175–192. https://doi.org/10.1016/0012-821X(87)90154-3

Ellison, C. R., Chapman, M. R., & Hall, I. R. (2006). Surface and deep ocean interactions during the cold climate event 8200 years ago. *Science*, *312*, 1929–1932. https://doi.org/10.1126/science.1127213

Gupta, A. K., Anderson, D. M., & Overpeck, J. T. (2003). Abrupt changes in the Asian southwest monsoon during the Holocene and their links to the North Atlantic Ocean. *Nature, 421*(6921), 354–357. https://doi.org/10.1038/nature01340

Hersbach, H., Bell, B., Berrisford, P., Hirahara, S., Horányi, A., Muñoz-Sabater, J., et al. (2020). The ERA5 global reanalysis. *Quarterly Journal of the Royal Meteorological Society*, *146*, 1999–2049. https://doi.org/10.1002/qj.3803

Hu, J., Emile-Geay, J., Tabor, C., Nusbaumer, J., & Partin, J. (2019). Deciphering oxygen isotope records from Chinese speleothems with an isotope-enabled climate model. *Paleoceanography and Paleoclimatology, 34*(12), 2098–2112. https://doi.org/10.1029/2019PA003741

Hughen, K. A., Overpeck, J. T., Peterson, L. C., & Trumbore, S. (1996). Rapid climate changes in the tropical Atlantic region during the last deglaciation. *Nature*, *380*, 51–54. https://doi.org/10.1038/380051a0

Jennings, A., Andrews, J., Pearce, C., Wilson, L., & Ólfasdótttir, S. (2015). Detrital carbonate peaks on the Labrador shelf, a 13–7 ka template for freshwater forcing from the Hudson Strait outlet of the Laurentide Ice Sheet into the subpolar gyre. *Quaternary Science Reviews, 107*, 62–80. https://doi.org/10.1016/j.quascirev.2014.10.022

Kerr, R. A. (2000). A North Atlantic climate pacemaker for the centuries. *Science, 288*(5473), 1984–1985. https://doi.org/10.1126/science.288.5473.1984

Lei, L., Xing, N., Zhou, X., Sun, J., Zhai, L., Jing, H., & Guo, J. (2020). A study on the warm-sector torrential rainfall during 15—16 July 2018 in Beijing area. *Acta Meteorologica Sinica, 78*, 1–17. (in Chinese)

Li, X., Cheng, H., Tan, L., Ban, F., Sinha, A., Duan, W., et al. (2017). The East Asian summer monsoon variability over the last 145 years inferred from the Shihua Cave record, North China. *Scientific Reports, 7*, 7078. https://doi.org/10.1038/s41598-017-07251-3

Liu, D., Wang, Y., Cheng, H., Edwards, R. L., & Kong, X. (2015). Cyclic changes of Asian monsoon intensity during the early mid-Holocene from annually-laminated stalagmites, central China. *Quaternary Science Reviews, 121*, 1–10. https://doi.org/10.1016/j.quascirev.2015.05.003

Liu, Y., Henderson, G. M., Hu, C., Mason, A. J., Charnley, N., Johnson, K. R., et al. (2013). Links between the East Asian monsoon and north Atlantic climate during the 8,200 year event. *Nature Geoscience, 6*, 117–120. https://doi.org/10.1038/ngeo1708.

Liu, Y., & Hu, C. (2016). Quantification of southwest China rainfall during the 8.2 ka BP event with response to North Atlantic cooling. *Climate of the Past, 12*(7), 1583–1590. https://doi.org/10.5194/cp-12-1583-2016

Ma, Z., Cheng, H., Tan, M., Edwards, R. L., Li, H., You, C., et al. (2012). Timing and structure of the Younger Dryas event in northern China. *Quaternary Science Reviews, 41*, 83–93. https://doi.org/10.1016/j.quascirev.2012.03.006

Mantua, N. J., Hare, S. R., Zhang, Y., Wallace, J. M., & Francis, R. C. (1997). A Pacific interdecadal climate oscillation with impacts on salmon production. *Bulletin of the american Meteorological Society, 78*(6), 1069–1080. https://doi.org/10.1175/1520-0477(1997)078<1069:APICOW>2.0.CO;2

Markle, B. R., Steig, E. J., Buizert, C., Schoenemann, S. W., Bitz, C. M., Fudge, T. J., et al. (2017). Global atmospheric teleconnections during Dansgaard-Oeschger events. *Nature Geoscience, 10*(1), 36–40. https://doi.org/10.1038/NGEO2848

Matero, I. S. O., Gregoire, L. J., Ivanovic, R. F., Tindall, J. C., & Haywood, A. M. (2017). The 8.2 ka cooling event caused by Laurentide ice saddle collapse. *Earth Planet Science Letters, 473*, 205–214. https://doi.org/10.1016/j.epsl.2017.06.011

Morrill, C., Anderson, D. M., Bauer, B. A., Buckner, R., Gille, E. P., Gross, W. S., et al. (2013). Proxy benchmarks for intercomparison of 8.2 ka simulations. *Climate of the Past, 9*, 423–432. https://doi.org/10.5194/cp-9-423-2013

Peros, M., Collins, S., G'Meiner, A. A., Reinhardt, E., & Pupo, F. M. (2017). Multistage 8.2 kyr event revealed through high-resolution XRF core scanning

of Cuban sinkhole sediments. *Geophysical Research Letters, 44*, 7374–7381. https://doi.org/10.1002/2017GL074369

Qian, C., & Zhou, T. (2014). Multidecadal variability of North China aridity and its relationship to PDO during 1900–2010. *Journal of Climate, 27*, 1210–1222, https://doi.org/10.1175/JCLI-D-13-00235.1

Rasmussen, S. O., Bigler, M., Blockley, S. P., Blunier, T., Buchardt, S. L., Clausen, H. B., et al. (2014). A stratigraphic framework for abrupt climatic changes during the Last Glacial period based on three synchronized Greenland ice-core records: refining and extending the INTIMATE event stratigraphy. *Quaternary Science Reviews, 106*, 14–28. http://dx.doi.org/10.1016/j.quascirev.2014.09.007

Ruth, U., Bigler, M., Röthlisberger, R., Siggaard-Andersen, M. L., Kipfstuhl, S., Goto-Azuma, K., et al. (2007). Ice core evidence for a very tight link between North Atlantic and east Asian glacial climate. *Geophysical Research Letters, 34*(3), L03706. https://doi.org/10.1029/2006GL027876

Schneider, T., Bischoff, T., & Haug, G. H. (2014). Migrations and dynamics of the intertropical convergence zone. *Nature, 513*(7516), 45–53. https://doi.org/10.1038/nature13636

Tan, L., Li, Y., Wang, X., Cai, Y., Lin, F., Cheng, H., et al. (2020). Holocene monsoon changes and abrupt events on the western Chinese Loess Plateau as revealed by accurately dated stalagmites. *Geophysical Research Letters, 47*, e2020GL090273. https://doi.org/10.1029/2020GL090273

Tan, M. (2014). Circulation effect: response of precipitation ^{18}O to the ENSO cycle in monsoon regions of China. *Climate Dynamics, 42*(3), 1067–1077. https://doi.org/10.1007/s00382-013-1732-x

Thomas, E. R., Wolff, E. W., Mulvaney, R., Steffensen, J. P., Johnsen, S. J., Arrowsmith, C., et al. (2007). The 8.2 ka event from Greenland ice cores. *Quaternary Science Reviews, 26*, 70–81. https://doi.org/10.1016/j.quascirev.2006.07.017

Wagner, A. J., Morrill, C., Otto-Bliesner, B. L., Rosenbloom, N., & Watkins, K. R. (2013). Model support for forcing of the 8.2 ka event by meltwater from the Hudson Bay ice dome. *Climate dynamics, 41*(11–12), 2855–2873. https://doi.org/10.1007/s00382-013-1706-z

Wang, P. X., Wang, B., Cheng, H., Fasullo, J., Guo, Z., Kiefer, T., & Liu, Z. (2017). The global monsoon across time scales: Mechanisms and outstanding issues. *Earth-Science Reviews, 174*, 84-121. http://dx.doi.org/10.1016/j.earscirev.2017.07.006

Wu, J. Y., Wang, Y. J., Cheng, H., Kong, X. G., & Liu, D. B. (2012). Stable isotope and trace element investigation of two contemporaneous annually-laminated stalagmites from northeastern China surrounding the" 8.2 ka event". *Climate of the Past, 8*(5), 1497–1507. https://doi.org/10.5194/cp-8-1497-2012

Yoshimura, K., Kanamitsu, M., Noone, D., & Oki, T. (2008). Historical isotope simulation using reanalysis atmospheric data. *Journal of Geophysical Research: Atmospheres, 113*, D19108. https://doi.org/10.1029/2008JD010074

Yu, L. (2013). Potential correlation between the decadal East Asian summer monsoon variability and the Pacific Decadal Oscillation. *Atmosphere Ocean Scientific Letters, 5*, 394–497. https://doi.org/10.3878/j.issn.1674-2834.13.0040

Zhang, H., Cheng, H., Spötl, C., Zhang, X., Cruz, F. W., Sinha, A., et al. (2021a). Gradual South-North Climate Transition in the Atlantic Realm Within the Younger Dryas. *Geophysical Research Letters, 48*(8), e2021GL092620. https://doi.org/10.1029/2021GL092620

Zhang, H., Zhang, X., Cai, Y., Sinha, A., Spötl, C., Baker, J., Cheng, H., et al. (2021b). A data-model comparison pinpoints Holocene spatiotemporal pattern of East Asian summer monsoon. *Quaternary Science Reviews, 261*, 106911. https://doi.org/10.1016/j.quascirev.2021.106911

Zhang, R., & Delworth, T. L. (2005). Simulated tropical response to a substantial weakening of the Atlantic thermohaline circulation. *Journal of Climate, 18*(12), 1853–1860. https://doi.org/10.1175/JCLI3460.1

Zhao, J., & Cheng, H. (2017). Applications of laser scanning confocal microscope to paleoclimate research: Characterizing and counting laminae. *Quaternary Sciences*, *37*, 1472–1474. (in Chinese).

Zhao, J., Cheng, H., Yang, Y., Tan, L., Spötl, C., Ning, Y., et al. (2019). Reconstructing the western boundary variability of the Western Pacific Subtropical High over the past 200 years via Chinese cave oxygen isotope records. *Climate Dynamics, 52*(5), 3741–3757. https://doi.org/10.1007/s00382-018-4456-0.

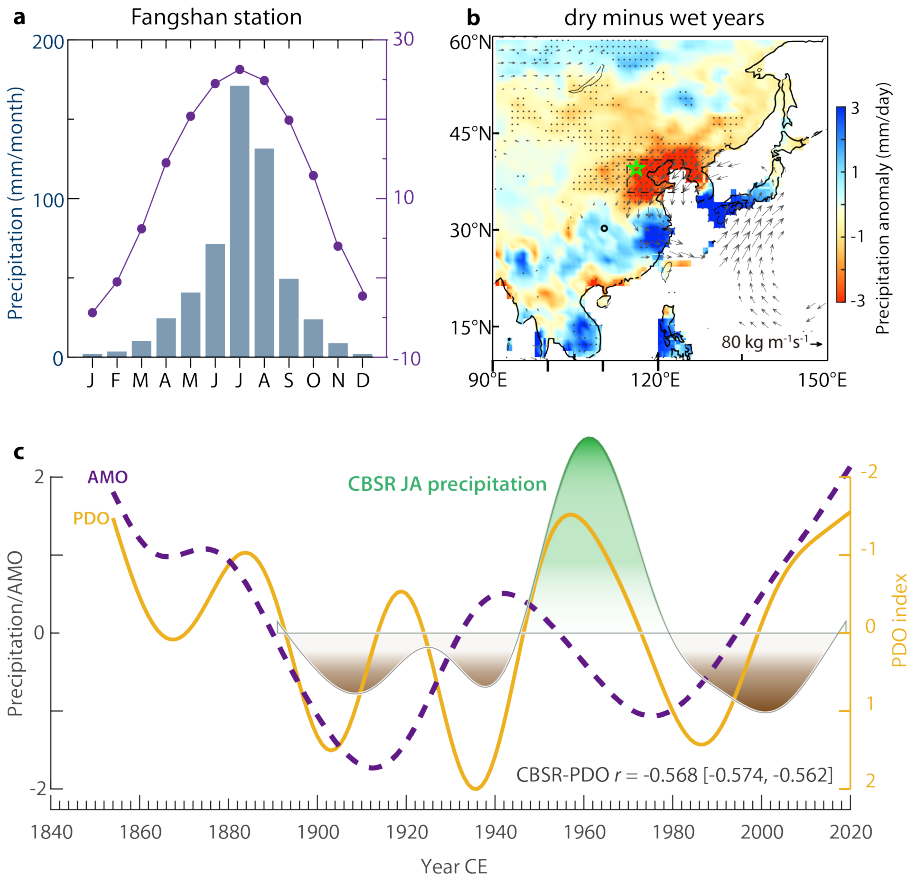

Figure 1. Regional climatology and location map. (**a**) Climographs of precipitation (blue bars) and temperature (purple dots and line) at Fangshan Station (39°46 N, 116°28 E) nearby Huangyuan Cave (data from Chinese Meteorological Administration, http://www.cma.gov.cn/). (**b**) Anomalies between dry and wet years (see details in Figure S5) for July and August (JA) precipitation (shading) and water vapor flux (arrow) based on the European Centre for Medium-Range Weather Forecasts Reanalysis fifth-generation dataset (ERA5) (Hersbach et al., 2020). Stippling and arrows indicate significant differences at 90 % confidence level. Green star and dashed black rectangle represent the locations of Huangyuan Cave and CBSR, respectively. Black circle indicates Heshang Cave. (**c**) The z-scored JA precipitation over the CBSR is 10 year-low pass filtered and shaded with green and brown for pluvial and dry periods. 10 year-low pass filtered PDO (yellow) (Mantua et al., 1997) and AMO (purple dash) (Kerr, 2000) indexes are shown.

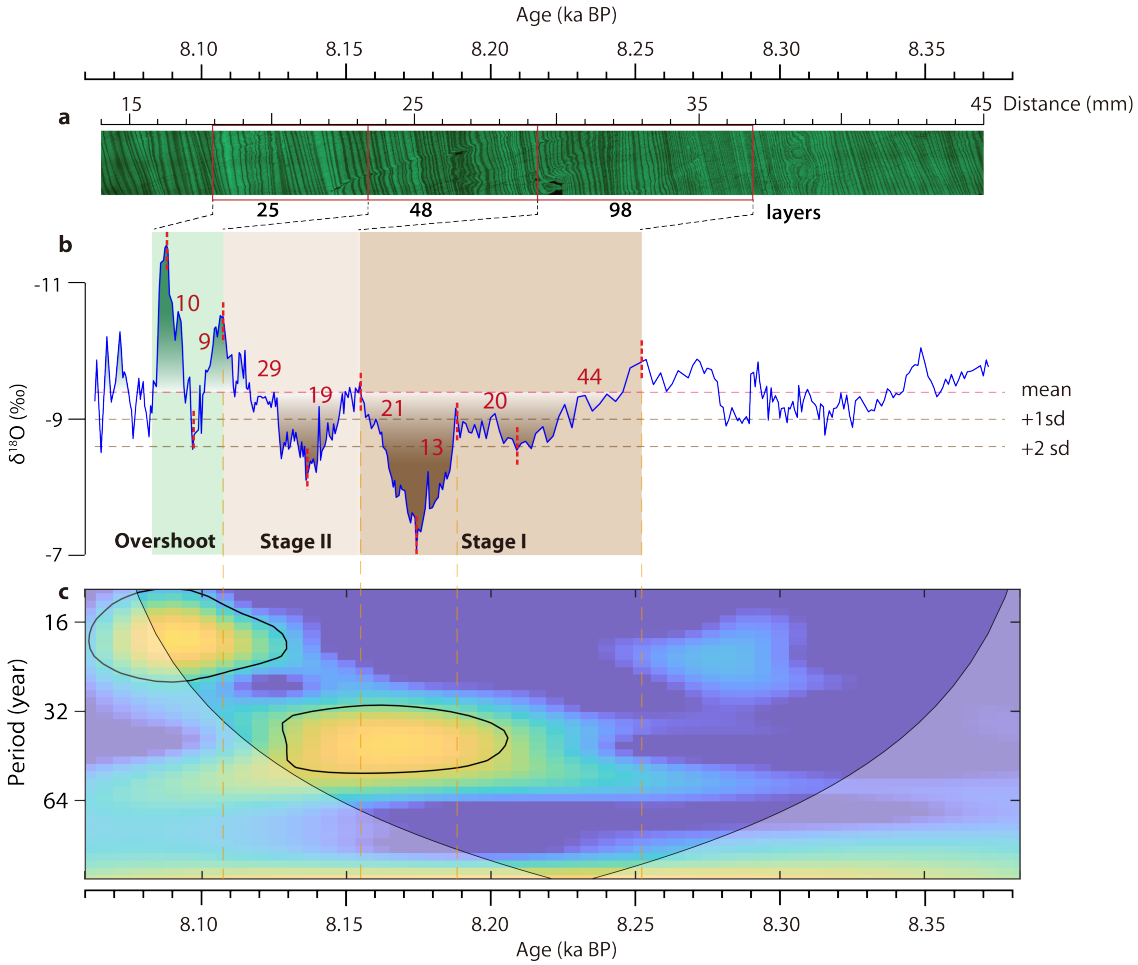

Figure 2. The BH-2 ^{18}O record of the 8.2 ka event. (**a**) The confocal scanning image of speleothem BH-2 between 13.5–45 mm in distance scale. (**b**) The BH-2 ^{18}O record between 8.38 and 8.06 ka BP. The horizontal dashed lines indicate the mean value (red), and +1 and +2 standard deviation (gray) of the whole record. The two-stage structure of the 8.2 ka event and overshoot periods are marked by vertical shading bars and their corresponding layers are highlighted by red rectangles in (**a**) and layer counts are shown with red number. (**c**) Continuous wavelet transform analysis of the BH-2 ^{18}O record. The 90 % significance level against red noise is shown as a thick contour. The edge effects of wavelet analysis are shaded in cone.

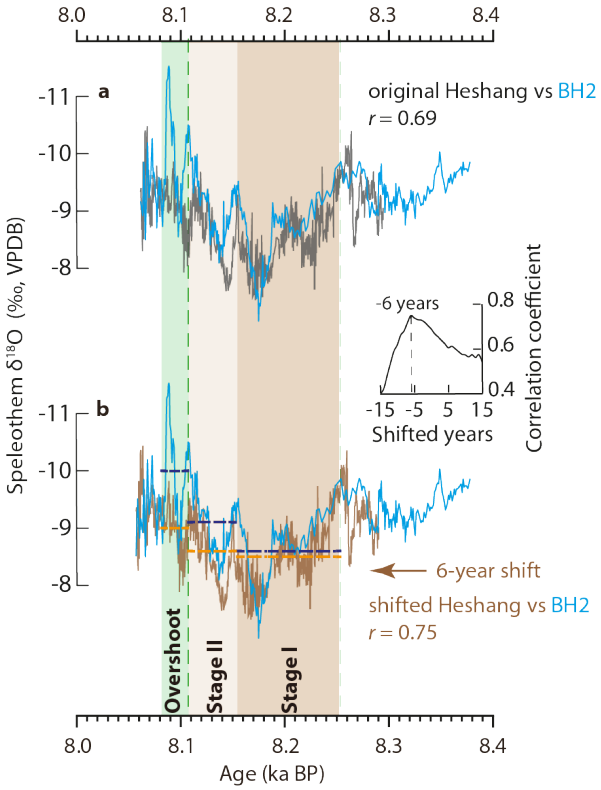

Figure 3. Comparison between the Huangyuan (BH-2) and Heshang (HS-4) ^{18}O records. (**a**) Comparison between original HS-4 (gray) (Liu et al., 2013) and BH-2 (blue, this study) ^{18}O records across the 8.2 ka event. (**b**) Comparison between the -6 year shifted HS-4 (brown) and BH-2 (blue) ^{18}O records. The horizontal dash lines (BH-2: dark blue; HS-4: khaki) represent the average ^{18}O values in the three periods, respectively. Vertical shading bars mark the Stage I, Stage II and overshoot intervals, respectively. The inset at the middle right indicates the correlation coefficient between HS-4 and BH-2 ^{18}O records by shifting the chronology of the HS-4 record.

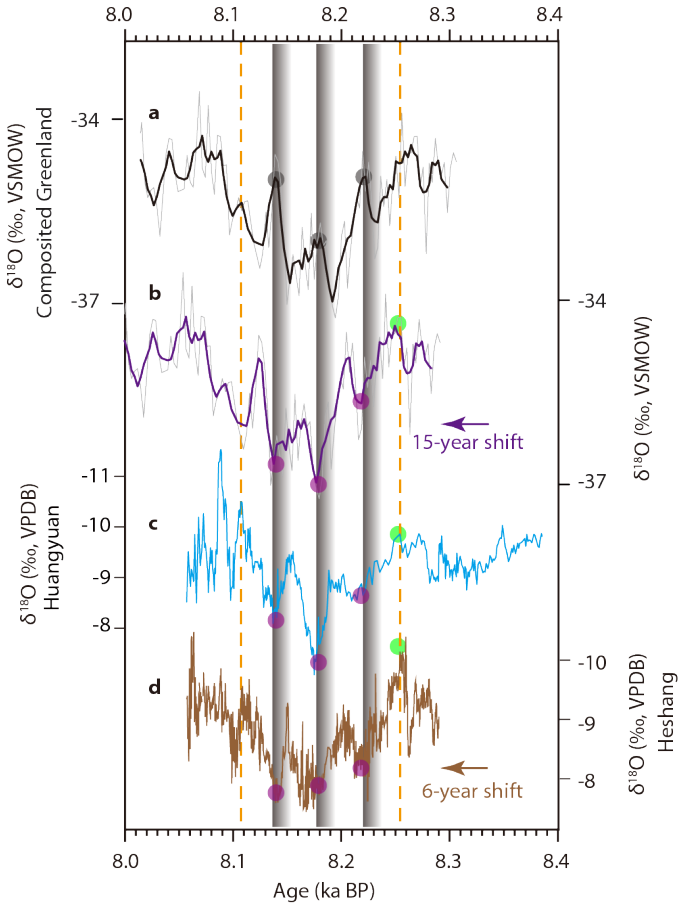

Figure 4. Comparison of ^{18}O records between speleothems BH-2, HS-4 and Greenland ice cores. (**a**) The original (gray) and 10-year moving averaged (black) ^{18}O records of the 8.2 ka event of Greenland ice cores (Thomas et al., 2007). (**b**) The same as (**a**) but with a -15-year shift. (**c**) The ^{18}O record of BH-2. (**d**) The -6 years shifted ^{18}O record of HS-4. Purple dots in each record, in combination with the vertical shading bars, mark the three "V-shape" excursions in Greenland, BH-2 and HS-4 records. In contrast, the gray dots in (**a**) show peaks in the Original Greenland ice core records, correlated apparently the "V-shape" excursions in the BH-2 record (**c**). The green dots in (**b c**) indicate the onset of the 8.2 ka event. The vertical yellow dash lines cover the duration of the 8.2 ka event revealed by the BH-2 ^{18}O record.